

## Supplementary Information

### **Characterization of Silver Ion Dissolution from Silver Nanoparticles using Fluorous-phase Ion-selective Electrodes and Assessment of Resultant Toxicity to *Shewanella oneidensis***

Melissa A. Maurer-Jones,<sup>†</sup> Maral P.S. Mousavi,<sup>†</sup> Li D. Chen, Philippe Bühlmann\* and Christy L. Haynes\*

Department of Chemistry, University of Minnesota, 207 Pleasant St SE, Minneapolis, MN 55455, United States of America

Fax: 612-626-7541; Tel: 612-626-1096; Email: [chaynes@umn.edu](mailto:chaynes@umn.edu), [buhlmann@umn.edu](mailto:buhlmann@umn.edu)

<sup>†</sup> These authors contributed equally to this work.

## Experimental Methods

### Nanoparticle Synthesis and Characterization

Citrate-capped Ag NPs were synthesized freshly for every experiment following a procedure detailed by Hackley and coworkers.<sup>1</sup> Prior to synthesis, glassware was cleaned with aqua regia (3:1 HCl:HNO<sub>3</sub>) and rinsed three times with deionized purified water (18MΩ·cm specific resistance, EMD Millipore, Burlington, MA, USA). For the synthesis, 50 mL deionized water was brought to a boil and then 365 μL of 34 mM trisodium citrate dihydrate (Sigma Aldrich, St. Louis, MO, USA) and 211 μL AgNO<sub>3</sub> (Sigma Aldrich) were added, followed by drop-wise addition of freshly prepared 250 μL NaBH<sub>4</sub> (Sigma Aldrich). Upon addition of NaBH<sub>4</sub>, the solution immediately turned yellow, and the mixture was allowed to boil for 15 min before removing the nanoparticles from heat and allowing them to come to room temperature. Nanoparticles were purified with regenerated cellulose (MWC0 50,000) centrifugal filter units (EMD Millipore) where 15 mL of the nanoparticle suspension were centrifuged at 1500 g for 4 min and then resuspended in deionized water, with the centrifuge/resuspension steps repeated in triplicate. The concentration of nanoparticles in the final, purified nanoparticle solution was determined with UV-visible spectroscopy (USB2000, Ocean Optics, Dunedin, FL, USA) using the extinction coefficient  $8.7 \times 10^8 \text{ M}^{-1} \text{ cm}^{-1}$ , as determined experimentally via correlation of absorbance values to concentrations of nanoparticles measured with ICP-MS (ICP-MS method below). Nanoparticle concentrations were converted to μg/mL by calculating the number of atoms per nanoparticle and converting atoms to mass using the atomic weight of Ag. The number of atoms per nanoparticle (*U*) were determined based on Equation 1 from Marquis et al.<sup>2</sup>

$$U \approx \frac{2}{3} \left(\frac{D}{a}\right)^3 \quad (1)$$

where *D* is the nanoparticle diameter (11 nm) and *a* is the edge length of the unit cell (4.0857 Å for Ag).

Nanoparticles were characterized by transmission electron microscopy (TEM – JEOL 1200EX III, JEOL, Tokyo, Japan), UV-visible spectroscopy (USB2000, Ocean Optics), dynamic light scattering (DLS – 90Plus, Brookhaven Instruments), and ζ-potential measurement (ZetaPALS, Brookhaven Instruments). The stability of the nanoparticles was monitored over 24 h with both DLS and ζ-potential in both deionized water and bacterial ferric citrate medium (described below).

### Fluorous-phase Ion-selective Electrode Fabrication

Ionophore-doped fluorous-phase ion-selective electrodes (ISEs) were prepared as reported previously.<sup>3</sup> To prepare the sensing phase, 0.5 mM ionic sites (sodium tetrakis[3,5-bis(perfluorohexyl)phenyl]borate) and 1.5 mM ionophore (1,3-bis(perfluorooctyl-ethylthio-methyl)benzene)<sup>4</sup> were added to perfluoroperhydrophenanthrene (Alfa Aesar, Ward Hill, MA, USA), and the resulting mixture was stirred for at least 24 h to ensure complete dissolution. Fluoropore™ filters (porous poly(tetrafluoroethylene), 47 mm diameter, 0.45 μm pore size, 50 μm thick, 85% porosity, EMD Millipore, Bedford, MA, USA) were sandwiched between two note cards, and cut with a 13 mm diameter hole punch, giving porous filter disks to mechanically support the sensing phase. Fluorous sensing phase was then applied with a micropipet to a stack of 2 porous filter disks. Full penetration of the fluorous phase into the porous supports was confirmed by a translucent appearance of the thus prepared sensing membranes.

The filter disks impregnated with fluororous sensing phase were then mounted into custom-machined electrode bodies made of poly(chlorotrifluoroethylene), as described previously.<sup>4</sup> In brief, a screw cap with a hole (8.3 mm diameter) in the center was screwed onto the electrode body, mechanically securing the sensing membrane in between the electrode body and the cap but leaving the center of the membrane exposed. The electrode bodies were then filled with 1  $\mu\text{M}$   $\text{AgCH}_3\text{CO}_2$  (Sigma Aldrich, USA) for studies in bacterial growth medium or with 1  $\mu\text{M}$   $\text{AgNO}_3$  for studies in water, and a  $\text{AgCl}/\text{Ag}$  inner reference electrode was inserted into this inner solution. Prior to measurements with bacterial growth medium, all electrodes were conditioned first for 24 h in 100 mL 0.1 mM  $\text{AgCH}_3\text{CO}_2$  solution ( $\text{AgNO}_3$  for studies in water) and then for another 24 h in 100 mL 1.0  $\mu\text{M}$   $\text{AgCH}_3\text{CO}_2$  ( $\text{AgNO}_3$  for studies in water). The same salt of silver was used for the inner filling and conditioning solutions.

### Fluororous-phase ISE Measurements

Potentials were monitored with an EMF 16 potentiometer (Lawson Labs, Malvern, PA, USA) controlled with EMF Suite 1.02 software (Lawson Labs) at room temperature (25 °C) in stirred solutions. The external reference electrode consisted of a double-junction  $\text{AgCl}/\text{Ag}$  electrode with a 1.0 M  $\text{LiOAc}$  bridge electrolyte and a 3.0 M  $\text{KCl}$  reference electrolyte. All measurements were performed with 3 replicate electrodes. For studies in water, calibration curves were obtained by successive dilution of a 10 mM  $\text{AgNO}_3$  solution with water. For studies in bacterial growth medium, calibration curves were obtained by addition of various volumes of 10 mM  $\text{AgCH}_3\text{CO}_2$  to 100 mL water or culture medium. To monitor the dissolution of nanoparticles over 24 h, 3 electrodes were prepared, calibrated, and placed in 100 mL of the solution of interest. Purified Ag NPs as described above were added to give varying Ag NP concentrations (0.3–15  $\mu\text{g}/\text{mL}$ ), and the EMF was monitored for 24 hours, after which the electrodes were again calibrated to ensure stability of response and sensitivity to  $\text{Ag}^+$ . Ag NP dissolution was monitored in water and ferric citrate bacterial growth medium.

### Bacterial Growth Media

Ferric citrate media for bacterial culture was prepared with a much lower chloride content than previously reported in the literature<sup>5</sup> to prevent  $\text{AgCl}$  precipitation. It consisted of 56 mM ferric citrate (Sigma Aldrich), 30 mM sodium lactate (from 60% solution, Spectrum Chemical, Redondo Beach, CA, USA), 30 mM  $\text{NaHCO}_3$  (Sigma Aldrich), 5 mM  $\text{NaH}_2\text{PO}_4$  (Sigma Aldrich, St. Louis, MO, USA), 19 mM  $(\text{NH}_4)_2\text{SO}_4$  (Fisher Chemical, Fairlawn, NJ, USA), 1 mM  $\text{KCH}_3\text{CO}_2$  (Mallinckrodt, Phillipsburg, NJ, USA), and hundredfold diluted mineral stock solution (see details below). To make the growth medium, ferric citrate was dissolved in deionized water by mild heating, and then the pH was adjusted to 6.7 with  $\text{NaOH}$  (Mallinckrodt). Addition of the other components yielded a final pH of  $\approx 7.7$ . The mineral stock solution consisted of 17.3 mM  $\text{NaCH}_3\text{CO}_2$  (EMD, Gibbstown, NJ, USA), 8.7 mM  $\text{MnSO}_4 \cdot \text{H}_2\text{O}$  (Mallinckrodt), 0.9 mM  $\text{CaCl}_2$  (Fisher Chemical), 0.4 mM  $\text{CoCl}_2 \cdot 6\text{H}_2\text{O}$  (Mallinckrodt), 0.4 mM  $\text{FeSO}_4 \cdot 7\text{H}_2\text{O}$  (Fisher Chemical), 0.15 mM  $\text{H}_3\text{BO}_3$  (Mallinckrodt), 25  $\mu\text{M}$   $\text{AlK}(\text{SO}_4)_2 \cdot 12\text{H}_2\text{O}$  (Mallinckrodt), 46  $\mu\text{M}$   $\text{CuSO}_4 \cdot 5\text{H}_2\text{O}$  (Spectrum Chemical, Redondo Beach, CA, USA), and 41  $\mu\text{M}$   $\text{Na}_2\text{MoO}_4 \cdot 2\text{H}_2\text{O}$  (Sigma Aldrich).

## ICP-MS Studies

Ag NP dissolution in deionized water and ferric citrate growth medium was monitored at discrete time points in parallel experiments using ICP-MS (XSeries 2, Thermo Scientific, Beverly, MA, USA). In these experiments, aliquots were collected at 0, 2, 6, 12, and 24 h, and supernatants were separated from the nanoparticles by centrifugation at 4000 g for 10 min using centrifugal filter units. Supernatants were analyzed for m/z 107 for Ag quantitation, with an indium internal standard monitored at m/z 115. The concentrations of Ag NPs and Ag<sup>+</sup> ion are reported here with different units (µg/mL or M, respectively) so as to align with common literature practice.

## Bacterial Culture

*Shewanella oneidensis* MR-1 were generously gifted by the Gralnick lab at the University of Minnesota. To prepare bacteria for toxicity assessments, cells stored at -80 °C were streaked onto an agar plate, allowing colonies to grow for 18–24 h, upon which colonies were transferred to Luria-Bertani (LB) growth medium (1 colony per 5 mL medium). Cells were cultured to stationary phase overnight (over 15 h) on a shaking incubator (200 rpm at 30 °C), pelleted by centrifugation at 750 g for 10 min, and resuspended in the ferric citrate growth medium. This suspension of cells was used going forward for toxicity assessments, and is herein referred to as “bacteria suspension,” the cell density of which was consistently 10<sup>9</sup> cells/mL. When bacteria were not being used or measured, the suspension was placed on the shaking incubator.

## Bacterial Toxicity Assays

### Uptake and Association

Bacterial nanoparticle uptake/association, and/or *S. oneidensis* morphology changes as the result of exposure to Ag<sup>+</sup> and Ag NPs were assessed by TEM. The bacterial suspensions were diluted to 10<sup>8</sup> cells/mL, and cells were exposed to control, 3 µM Ag<sup>+</sup>, 3 µg/mL Ag NPs conditions for 24 h, after which, bacteria samples were prepared as previously described for mammalian cells.<sup>6</sup> Briefly, cells were pelleted by centrifugation at 500 g for 10 min and washed with 0.1 M sodium cacodylate buffer. Bacteria were fixed with 2.5% glutaraldehyde (Sigma Aldrich) in 0.1 M sodium cacodylate buffer for 1 h, followed by a post-fixation for 1 h in 1% osmium tetroxide (Sigma Aldrich). Samples were dehydrated in a series of ethanol washes with increasing percentages of ethanol, followed by propylene oxide and finally Epon Polybed 812 resin (Miller-Stephenson, Columbus, OH, USA). Resin was exchanged 5 times over 36 h to allow proper intercalation and cured for 24 h at 45 °C, followed by 60 °C for 24 h. A diamond knife was used to cut 60 nm sections with an ultramicrotome, and sections were collected on a Formvar-coated copper grid and imaged at 60 kV on a JEOL 1200 EXII TEM (JEOL, Tokyo, Japan).

## Viability

LIVE/DEAD<sup>®</sup> BacLight<sup>™</sup> (Life Technologies, Grand Island, NY, USA) was used to assess viability of *S. oneidensis* after exposure to varying concentrations of AgCH<sub>3</sub>CO<sub>2</sub> (referred to as Ag<sup>+</sup>) and Ag NPs for up to 24 h. Cells from the bacteria suspension were diluted to a density of 10<sup>8</sup> cells/mL with ferric citrate medium and exposed to varying concentrations of Ag<sup>+</sup> (1–10 µM) or Ag NPs (0.3–15 µg/mL), with each condition cultured in triplicate and periodic assessment of viability taken over the 24 h exposure. To perform the viability assay, the staining solution was prepared as specified by the manufacturer (kit L7012) and was comprised of 2

fluorescent dyes, where live cells were stained with membrane-permeable SYTO-9 and dead cells were stained with red fluorescent propidium iodide. Periodically, 0.5 mL aliquots of the samples were centrifuged at 500 g for 10 min, and pelleted cells were resuspended in HEPES (4-(2-hydroxyethyl)-1-piperazineethanesulfonic acid) buffer solution with mineral additives to avoid scattering by iron oxide precipitates formed in the ferric citrate medium. HEPES buffer with mineral additives consisted of 100 mM HEPES, 7.8 mM NaCH<sub>3</sub>CO<sub>2</sub>, 1.3 mM K<sub>2</sub>HPO<sub>4</sub>, 1.7 mM KH<sub>2</sub>PO<sub>4</sub>, 1.7 mM (NH<sub>4</sub>)<sub>2</sub>SO<sub>4</sub>, 1 mM MgSO<sub>4</sub>, 9.5 μM ZnCl<sub>2</sub>, 1.9 μM NiCl<sub>2</sub>, 0.5 μM Na<sub>2</sub>MoO<sub>4</sub>·2H<sub>2</sub>O, 0.4 μM Na<sub>2</sub>WO<sub>4</sub>, 0.2 μM AlK(SO<sub>4</sub>)<sub>2</sub>·12H<sub>2</sub>O, 1.8 μM FeSO<sub>4</sub>·7H<sub>2</sub>O, 13.5 μM MnSO<sub>4</sub>·H<sub>2</sub>O, 0.2 μM CuSO<sub>4</sub>·5H<sub>2</sub>O, and 3.25 μM CoSO<sub>4</sub>·7H<sub>2</sub>O adjusted to pH 7.2 with NaOH.<sup>7</sup> Equal aliquots of the staining solution and resuspended bacteria (100 μL:100 μL) were mixed, placed in a 96-well plate, and incubated for 15 min in the dark. Fluorescence intensity was measured on a Synergy 2 (Biotek, Winooski, VT, USA) multi-well plate-reader ( $\lambda_{\text{excitation}} = 485$  nm;  $\lambda_{\text{emission SYTO-9}} = 528$  nm and  $\lambda_{\text{emission propidium iodide}} = 630$  nm). Measurements were performed after 0, 2, 6, 12, and 24 h exposure, and results were analyzed by comparing the ratio of live cells (green fluorescence) to dead cells (red fluorescence) for the control and silver exposure conditions.

## Growth

The phases of bacterial growth (lag, exponential, and stationary phases) were monitored for *S. oneidensis* after exposure to varying concentrations of Ag<sup>+</sup> and Ag NPs. The bacterial suspension was diluted to 10<sup>7</sup> cells/mL in ferric citrate medium with exposure to 1–10 μM Ag<sup>+</sup>, 0.3–15 μg/mL Ag NPs, or water for the control, with each condition in triplicate. Growth was monitored over 48 h with periodic measurements of the optical density (OD) at  $\lambda=600$  nm with a Spectronic 20D spectrophotometer (Milton Roy Company, Ivyland, PA, USA). Manual inspection of each curve to determine the exponential phase of growth was performed, and the growth rate, in generations/h, was calculated using Equation 2, which is based on the classic model of binary fission.

$$\text{growth rate} = \frac{\log OD_2 - \log OD_1}{0.301 \cdot \Delta t_{2-1}} \quad (2)$$

## Calculations and Results

### Complexation of Ammonia with Ag<sup>+</sup>

Ammonium, one of the components of the ferric citrate bacterial growth medium, dissociates to ammonia and becomes available to form stable complexes with Ag<sup>+</sup> (formation constants of  $K_{f,1}=10^{3.24}$  and  $K_{f,2}=10^{3.81}$ ).<sup>8</sup> The pH of the bacterial growth medium was measured and found to be 7.9, independent of the concentration of Ag<sup>+</sup>. Using the dissociation equation and mass balance for ammonium (Equations 3 and 4), the concentration of ammonia in solution can be calculated, as described in the following.

$$\frac{a_{\text{NH}_3} a_{\text{H}^+}}{a_{\text{NH}_4^+}} = K_a \quad (3)$$

$$[\text{NH}_3] + [\text{NH}_4^+] = C_{\text{total, NH}_4^+} \quad (4)$$

Activity coefficients were calculated using the Debye-Hückel extended theory (Equations 5 and 6), where  $I$  is the ionic strength of the solution,  $z$  is the charge of ions,  $\alpha$  is the ion size parameter (0.76 Å for NH<sub>4</sub><sup>+</sup>)<sup>9</sup> and, at 25 °C, A and B are 0.509 and 0.328 Å<sup>-1</sup>, respectively.<sup>10</sup>

$$\log \gamma_{\pm} = \left| \frac{z_{+}}{z_{-}} \right| \log \gamma_{\pm} \quad (5)$$

$$\log \gamma_{\pm} = -\frac{A(z_{+} z_{-})\sqrt{I}}{1 + B\alpha\sqrt{I}} \quad (6)$$

Using the acid dissociation constant of  $10^{-9.244}$ ,<sup>11</sup> a total concentration of 38 mM for ammonium, and  $10^{-7.9}$  M for  $a_{H^{+}}$ , the concentration of ammonia in the bacterial growth medium with an ionic strength of 0.123 was calculated to be  $1.5 \times 10^{-3}$  M. By using the formation equations for the silver ammonia complexes (Equations 7 and 8) and the mass balance for all dissolved species containing silver, the percentages of all  $Ag^{+}$  species can be calculated (see below). As an approximation, the activity coefficients of the complexed silver ions were assumed to be identical to those of the free  $Ag^{+}$ .

$$\frac{a_{AgNH_3^{+}}}{a_{Ag^{+}} a_{NH_3}} \cong \frac{[AgNH_3^{+}]}{[Ag^{+}][NH_3]} = K_{f,1} \quad (7)$$

$$\frac{a_{Ag(NH_3)_2^{+}}}{a_{AgNH_3^{+}} a_{NH_3}} \cong \frac{[Ag(NH_3)_2^{+}]}{[AgNH_3^{+}][NH_3]} = K_{f,2} \quad (8)$$

$$C_{total,Ag} = [Ag^{+}] + [AgNH_3^{+}] + [Ag(NH_3)_2^{+}] \quad (9)$$

Combining Equations 7, 8, and 9 gives Equation 10.

$$\begin{aligned} C_{total,Ag} &= [Ag^{+}] + [Ag^{+}][NH_3] K_{f,1} + [Ag^{+}][NH_3]^2 K_{f,1}K_{f,2} \\ &= [Ag^{+}] (1 + [NH_3] K_{f,1} + [NH_3]^2 K_{f,1}K_{f,2}) \end{aligned} \quad (10)$$

Equation 10 can be readily reformed to give the ratio of free silver ions and the total silver concentration. Using the known values of  $K_{f,1}$  and  $K_{f,2}$  and the activity of ammonia, this ratio is calculated as 0.033:

$$\frac{[Ag^{+}]}{C_{total,Ag}} = \frac{1}{(1 + [NH_3] K_{f,1} + [NH_3]^2 K_{f,1}K_{f,2})} = 0.033$$

The ratios of the silver complexes and the total silver concentrations can be obtained analogously:

$$\frac{[AgNH_3^{+}]}{C_{total,Ag}} = \frac{[NH_3] K_{f,1}}{(1 + [NH_3] K_{f,1} + [NH_3]^2 K_{f,1}K_{f,2})} = 0.089$$

$$\frac{[Ag(NH_3)_2^{+}]}{C_{total,Ag}} = \frac{[NH_3]^2 K_{f,1}K_{f,2}}{(1 + [NH_3] K_{f,1} + [NH_3]^2 K_{f,1}K_{f,2})} = 0.878$$

Thus, it can be concluded that 3.3% of total ionic silver species are in the form of free  $\text{Ag}^+$ , 8.9% are in the form of  $\text{AgNH}_3^+$ , and 87.8% are in the form of  $\text{Ag}(\text{NH}_3)_2^+$ .

### Effect of Ferric Citrate Components on the EMF Response

To investigate the effect of the individual components of the ferric citrate medium on the response of the  $\text{Ag}^+$  ISEs, solutions containing  $1\ \mu\text{M}$   $\text{AgCH}_3\text{CO}_2$ , and individual medium components ( $\text{MnSO}_4\cdot\text{H}_2\text{O}$ ,  $\text{CaCl}_2$ ,  $\text{CoCl}_2\cdot 6\text{H}_2\text{O}$ ,  $\text{FeSO}_4\cdot 7\text{H}_2\text{O}$ ,  $\text{H}_3\text{BO}_3$ ,  $\text{AlK}(\text{SO}_4)_2\cdot 12\text{H}_2\text{O}$ ,  $\text{CuSO}_4\cdot 5\text{H}_2\text{O}$ ,  $\text{Na}_2\text{MoO}_4\cdot 2\text{H}_2\text{O}$ ,  $\text{KCH}_3\text{CO}_2$ , and sodium lactate) were prepared, and the pH of the solutions was adjusted as for the ferric citrate medium by addition of sodium hydroxide or acetic acid. The electrodes were placed in 100 mL of  $1.0\ \mu\text{M}$   $\text{AgCH}_3\text{CO}_2$ , followed by step-by-step addition of known volumes of solutions of the ferric citrate medium components to make the final concentrations very similar to those in the complete ferric citrate medium. None of the species caused a significant change in the EMF, indicating that they do not interfere with the response and do not have any specific interaction with  $\text{Ag}^+$ . The average EMF changes for 3 replicate electrodes are shown in Table S1.

**Table S1.** Effect of broth components on EMF measurements. The electrodes were placed in 100 mL  $1.0\ \mu\text{M}$   $\text{AgCH}_3\text{CO}_2$  solution, followed by step-by-step addition of known volumes of solutions of the ferric citrate medium components to give final concentrations very similar to those in the ferric citrate medium.

	Concentration ( $\mu\text{M}$ )	Average change in EMF (mV)
$\text{AgCH}_3\text{CO}_2$	1.0	—
<i>After addition of:</i>		
$\text{H}_3\text{BO}_3$	1.5	$0.7 \pm 2.5$
$\text{Na}_2\text{MoO}_4$	0.41	$0.7 \pm 2.1$
$\text{CuSO}_4$	0.46	$-1.2 \pm 1.9$
$\text{AlK}(\text{SO}_4)_2$	0.25	$-1.1 \pm 1.1$
$\text{FeSO}_4$	4.0	$3.7 \pm 3.1$
$\text{CoCl}_2$	4.0	$0.8 \pm 4.4$
$\text{CaCl}_2$	9.0	$-3.3 \pm 4.0$
$\text{MnSO}_4$	87.0	$0.4 \pm 0.3$
$\text{NaCH}_3\text{CO}_2$	173.0	$1.5 \pm 3.5$
KOAc	1.0	$3.3 \pm 3.0$

In a similar experiment, less than 3 mV change in the EMF was observed after addition of 30 mM sodium lactate to ferric citrate medium containing 1  $\mu\text{M}$   $\text{AgCH}_3\text{CO}_2$ , indicating that in the ferric citrate medium there is no significant complexation between  $\text{Ag}^+$  and lactate anion.

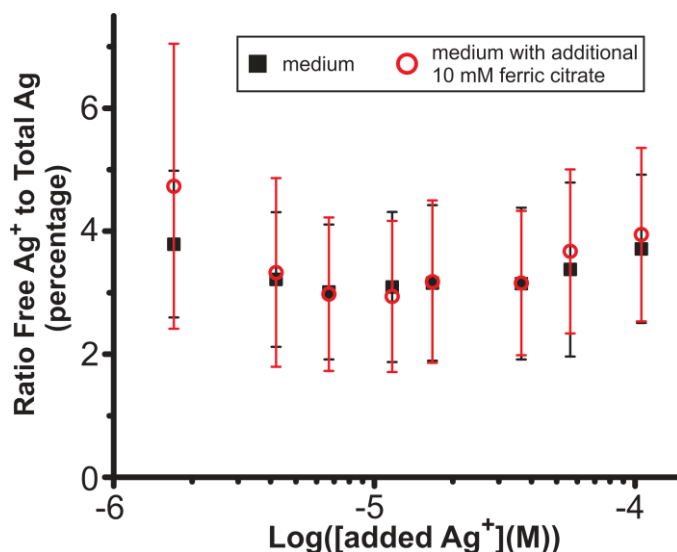


**Figure S1.** The  $\text{Ag}^+$ -selective ISEs do not show a significant difference between free  $\text{Ag}^+$  in ferric citrate medium and free  $\text{Ag}^+$  in ferric citrate medium with an additional 10 mM sodium citrate, confirming that citrate in ferric citrate medium does not affect the free  $\text{Ag}^+$  activity in this medium.

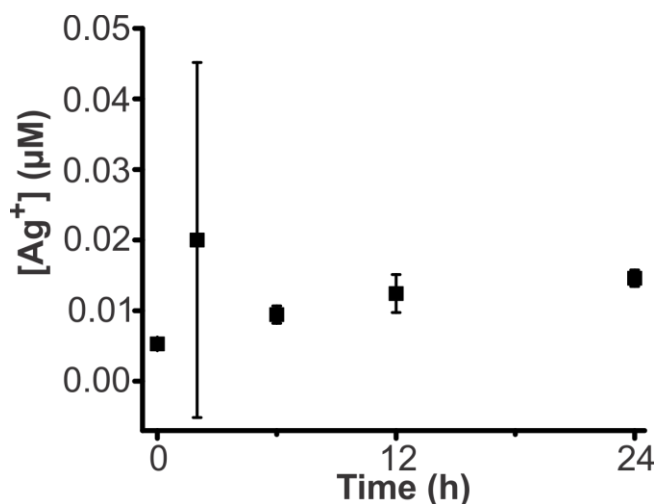


**Figure S2.** ICP-MS measurement over time of ferric citrate media spiked with 5  $\mu\text{M}$   $\text{AgCH}_3\text{CO}_2$  reveals that the ICP-MS sample preparation method causes a significant decrease in the  $\text{Ag}^+$ . The decrease may be due to adsorption of  $\text{Ag}^+$  onto the iron precipitate that commonly forms in the ferric citrate medium, which is filtered off in the ICP-MS sample preparation. This artifact further supports the need for in situ nanoparticle characterization such as the ISE employed herein.

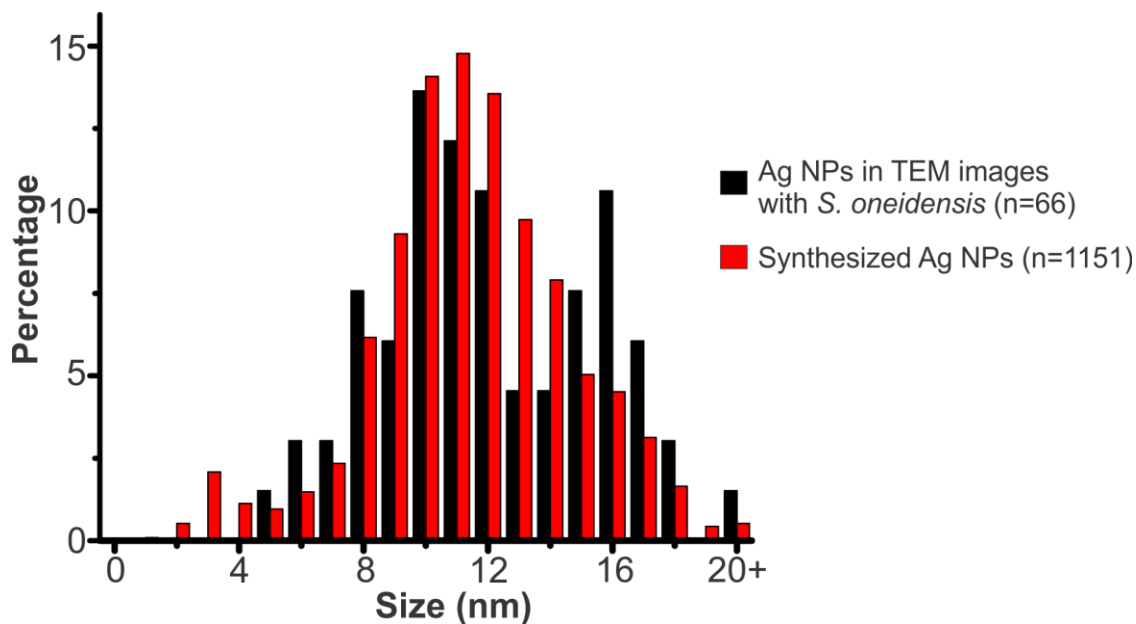


**Figure S3.** Histogram analysis of nanoparticle diameter found in proximity to bacteria (as seen in Figure 7B) as compared to the synthesized nanoparticle size distribution (as compiled from Figure 1B). The similarity of these distributions suggests that the nanoparticles near the bacteria are, in fact, the synthesized Ag nanoparticles.

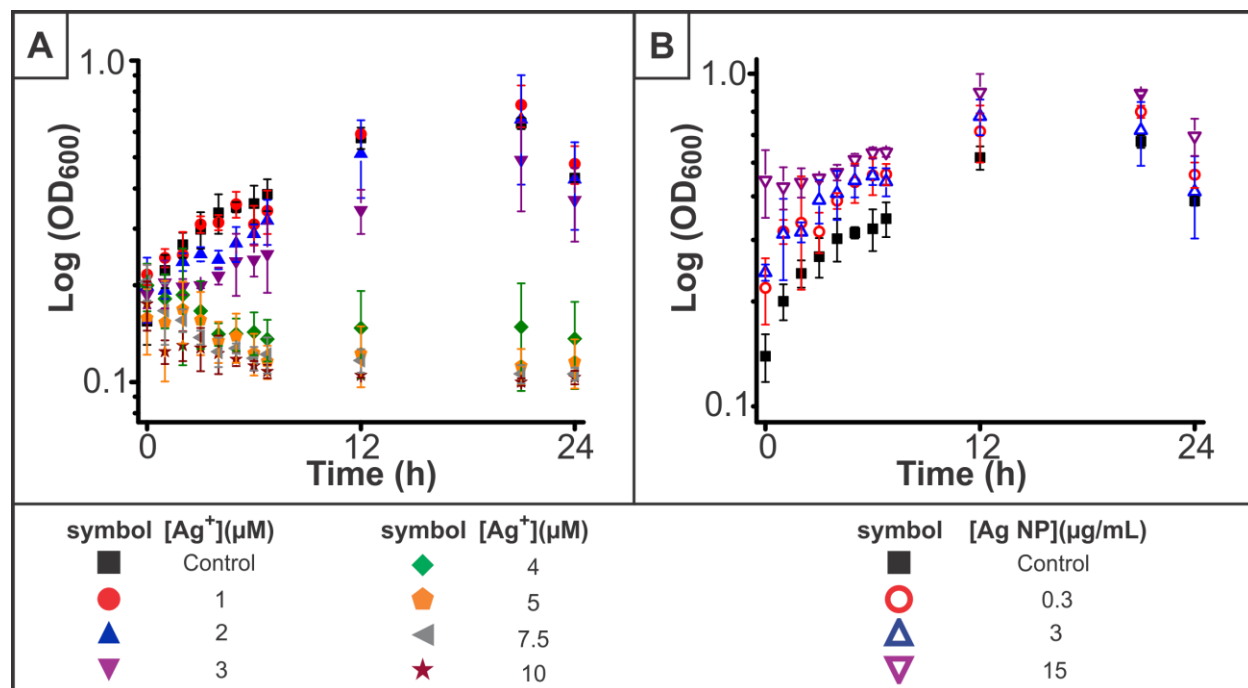


**Figure S4.** Growth curves for *S. oneidensis* in the presence of (A) Ag<sup>+</sup> or (B) Ag NPs.

**Table S3.** Growth rate of *S. oneidensis* exposed to Ag<sup>+</sup> or Ag NPs, as determined from the exponential growth phase in Figure S3, using Equation 2.

Concentration Ag NP (µg/mL)	Growth rate (generations/h)	Concentrations Ag <sup>+</sup> (µM)	Growth rate (generations/h)
Control	0.16	1	0.12
0.3	0.09	2	0.12
3	0.09	3	0.09
15	0.09	4, 5, 7.5, and 10	no growth

## References

1. S. L. Chinnapongse, R. I. MacCuspie and V. A. Hackley, *Sci. Total Environ.*, 2011, 409, 2443-2450.
2. B. J. Marquis, M. A. Maurer-Jones, K. L. Braun and C. L. Haynes, *Analyst*, 2009, 134, 2293-2300.
3. C.-Z. Lai, M. A. Fierke, R. C. a. d. Costa, J. A. Gladysz, A. Stein and P. Bühlmann, *Anal. Chem.*, 2010, 82, 7634-7640.
4. P. G. Boswell and P. Bühlmann, *J. Am. Chem. Soc.*, 2005, 127, 8958-8959.
5. R. M. Atlas, *Handbook of Microbiological Media*, 3<sup>rd</sup> Edition, CRC Press, Boca Raton, FL, 2004.
6. M. A. Maurer-Jones, Y.-S. Lin and C. L. Haynes, *ACS Nano*, 2010, 4, 3363-3373.
7. W. E. Balch, G. E. Fox, L. J. Magrum, C. R. Woese and R. S. Wolfe, *Microbiol. Rev.*, 1979, 43, 260-296.
8. J. A. Dean, *Lange's Handbook of Chemistry*, 14<sup>th</sup> Edition, McGraw-Hill, New York, NY, 1992.
9. J. Kielland, *J. Am. Chem. Soc.*, 1937, 59, 1675-1678.
10. W. E. Morf, *Studies in Analytical Chemistry, Vol. 2: The Principles of Ion-Selective Electrodes and of Membrane Transport*, Elsevier, New York, NY, 1981.
11. J. F. Rubinson and K. Rubinson, *Contemporary Chemical Analysis*, Prentice Hall, Upper Saddle River, NJ 1998.